Supplementary Figures for

Magnetite-rutile symplectite in ilmenite records magma hydration in layered intrusions

Wei Tan[1, 2, 3], Christina Yan Wang[1, 2], Steven M. Reddy[3, 4], Hongping He[1, 2]*, Haiyang Xian[1, 2], Changming Xing[1, 2]

[1]Key Laboratory of Mineralogy and Metallogeny, Guangdong Provincial Key Laboratory of Mineral Physics and Materials, Guangzhou Institute of Geochemistry, Chinese Academy of Sciences, Guangzhou 510640, China

[2]Institutions of Earth Science, Chinese Academy of Sciences, Beijing 100029, PR China

[3]School of Earth and Planetary Sciences, The Institute for Geoscience Research (TIGeR), Curtin University, GPO Box U1987, Perth, WA 6845, Australia

[4]Geoscience Atom Probe, Advanced Resource Characterisation Facility, John de Laeter Centre, Curtin University, GPO Box U1987, Perth, WA 6845, Australia

Introduction

The Supplementary Figures provides information to illustrate (1) elements distribution of nano-scale hematite lamellae in ilmenite; (2) HAAF-STEM/ HRTEM images showing nano-scale morphology and coherent interfaces of hematite lamellae in ilmenite; (3) Compositional ranges of the bulk compositions of ilmenite-hematite intergrowth, magnetite–rutile symplectite and the recasted composition including the two intergrowths within the FeO–Fe2O3–TiO2 diagram.

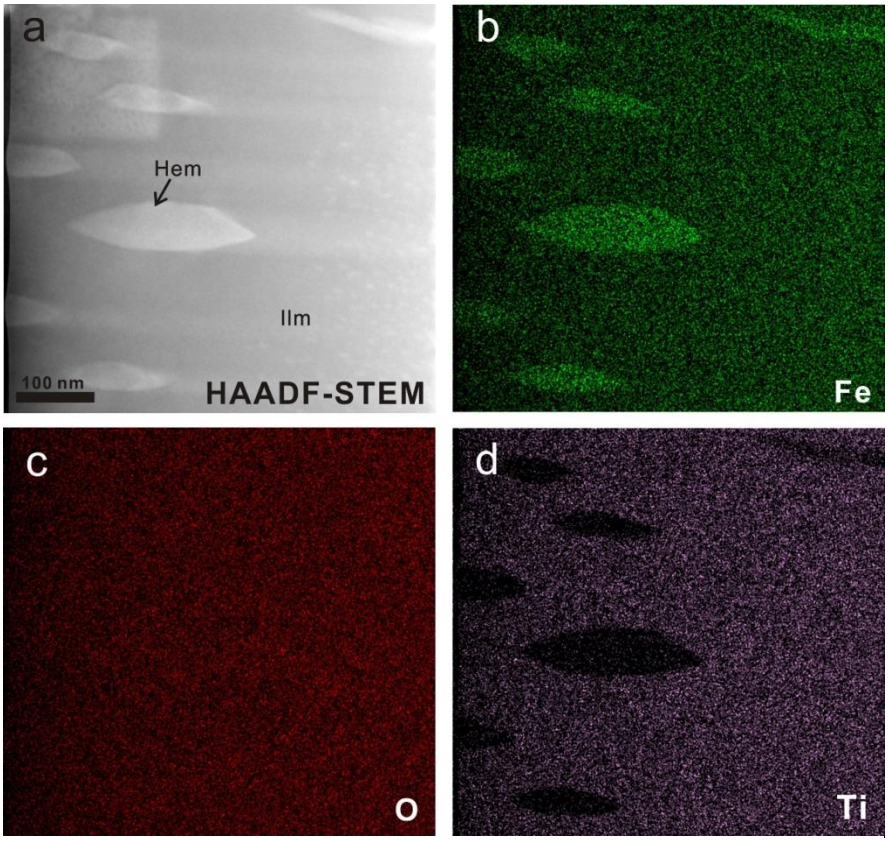

Fig. S1. Elements distribution of nano-scale hematite lamellae in ilmenite.
(a) High-angle annular dark-field scanning transmission electron microscope (HAAF-STEM) image showing the lens-like morphology of hematite lamellae in ilmenite; **(b-d)** The STEM-EDS mappings showing the distributions of Fe, O, Ti, in the area of interest.

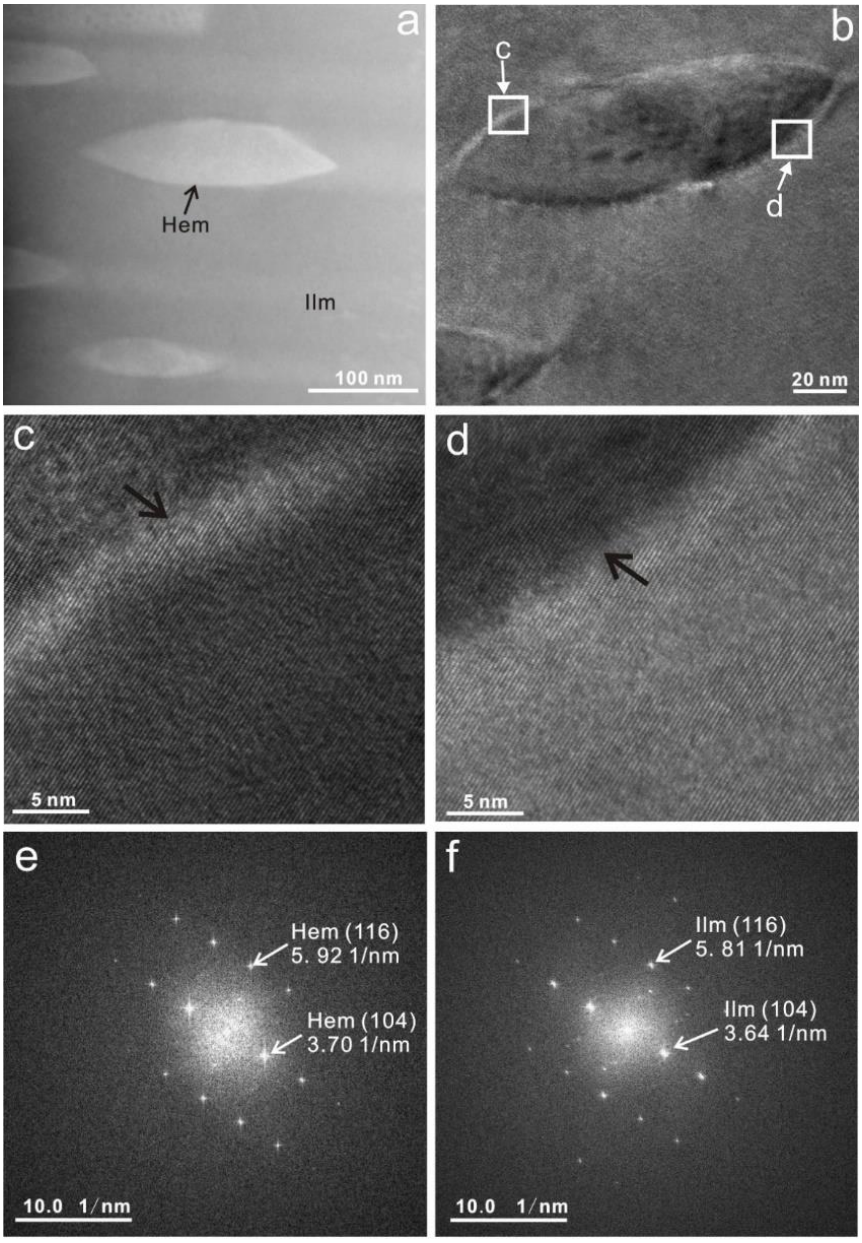

Fig. S2. HAAF-STEM/ HRTEM images showing nano-scale morphology and coherent interfaces of hematite lamellae in ilmenite.

(a) The HAAF-STEM image showing the area of interest; **(b)** TEM image of a hematite lamellar in ilmenite, white squares indicate the analysis areas shown in **c** and **d**; **(c)** High-resolution TEM image showing the top left corner of the hematite lamellar in **b**; **(d)** High-resolution TEM image showing the bottom right corner of the hematite lamellar in **b**; **(e)** Fourier transform diagram of the areas of the hematite lamellae in **c**; **(f)** Fourier transform diagram of the areas of the host ilmenite in **d**. Note: the black arrows in **c** and **d** point to the ilmenite-hematite coherent interfaces; the d-spacing data calculated based on the Fourier transform diagrams of the hematite lamellae are 2.70 Å for the (1 0 4) plane, and 1.69 Å for the (1 1 6) plane in **e**, and the host ilmenite 2.74 Å for the (1 0 4) plane, and 1.72 Å for the (1 1 6) plane in **f**, respectively.

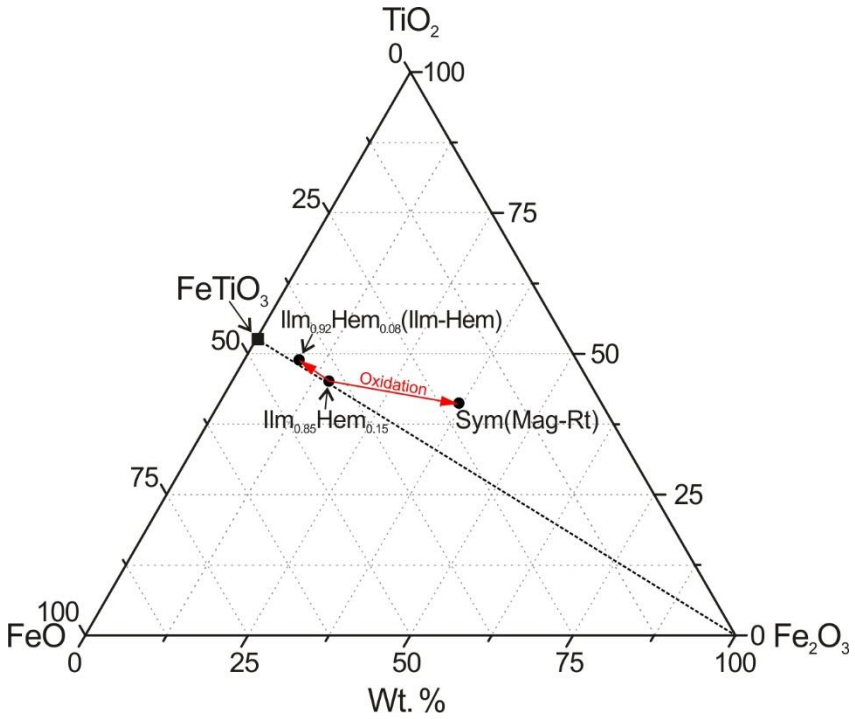

Fig. S3. Compositional ranges of the bulk compositions of ilmenite-hematite intergrowth, magnetite–rutile symplectite and the recasted composition including the two intergrowths within the $FeO–Fe_2O_3–TiO_2$ diagram.